JOURNAL OF GEOPHYSICAL RESEARCH, VOL. 100, NO. D8, PAGES 16,639–16,650, AUGUST 20, 1995

Aerosol optical depth over the oceans: Analysis in terms of synoptic air mass types

A. Smirnov, Y. Villevalde,[1] N.T. O'Neill, A. Royer, and A. Tarussov

Centre d'Applications et de Recherches en Télédétection, Université de Sherbrooke, Sherhrooke, Québec, Canada

Abstract. The results of spectral aerosol optical depth measurements in the Pacific Ocean, Baltic Sea, and North Atlantic are considered with regard to air mass types. It is found that the optical properties of continental and maritime air mass types differ significantly for the data employed in this study. A synoptical air mass context was also employed in demonstrating the correlation between near infrared aerosol optical depth τ_a(1640 nm) and wind speed as well as for investigations into the relationship between deck level relative humidity and the aerosol optical depth at 550 nm. Simulations, employing well-known aerosol parameterization models, of the aerosol optical depth spectra for various air mass types show good agreement with the experimental results in the visible and near infrared range.

Introduction

Comprehensive studies wherein one investigates the spatial and temporal links between optical depth variations and synoptic air mass parameters over the oceans is of great importance if we are to understand the mechanisms which define the optical state of the atmosphere. The results of these investigations are of interest in pure atmospheric optics as well as to such disciplines as remote sensing where the atmospheric optical state is an essential element in the radiometric calibration procedure of surface images. Spatial and temporal information extracted from aerosol optical measurements is required in radiative climatological applications such as those which focus on the refinement of general circulation models.

Relationships between air mass type and its optical characteristics in a maritime atmosphere have been studied by a number of researchers [*Von Hoyningen-Huene and Raabe*, 1987; *Weller and Leiterer*, 1988; *Hoppel et al.*, 1990; *Reddy et al.*, 1990; *Gulyaev et al.*, 1990; *Smirnov and Gulyaev*, 1990]. Some coastal measurements were recently considered by *Von Hoyningen-Huene and Wendisch* [1994]. Table 1 summarizes the known measurements of aerosol optical depth in oceanic and coastal areas for which air mass type analyses have been performed.

The results presented by *Von Hoyningen-Huene and Raabe* [1987], *Weller and Leiterer* [1988], *Gulyaev et al.* [1990], *Smirnov and Gulyaev* [1990], and *Von Hoyningen-Huene and Wendisch* [1994] followed a traditional air mass classification that asssumed the existence of two main fronts (polar and arctic), and thus three air mass types (arctic, polar, and tropical), with maritime and continental versions. The published optical classification results in Table 1 show a wide scatter of optical parameters in general and some significant scatter between the optical data for similar air mass types in particular. In spite of this scatter the table is indicative of the potential for coarse discrimination of optical parameters based on traditional synoptical air mass analysis. As obvious but relevant illustrations of this potential we would note the typically higher value of the Angstrom parameter and aerosol optical depth values in continental air mass types as compared to maritime air mass types.

Synoptical air mass analysis is a traditional and standard classification approach which we feel is a simple but effective optical class discrimination technique. Although the study of atmospheric optical parameters in conjunction with air mass back trajectories analyses represents a more comprehensive approach, it arguably yields a detail of discrimination that exceeds the classification requirements for many atmospheric optical applications. In any case such techniques have been applied successfully in the past [*Hoppel et al.*, 1990; *Reddy et al.*, 1990] and indicate in a general sense the utility of air mass classification for optical characterization. As an example, one can observe that the results obtained by these two groups for the mean values of aerosol optical depth (τ_a) and Angstrom parameter (a) in remote Atlantic air are in a good agreement (Table 1). Their comment that the most variable optical conditions were obtained for continental air arriving from the U.S. coast is a relevant observation which we sought to confirm in terms of the synoptical air mass analysis presented in this paper.

As pointed out by *Penner et al.* [1994], the aerosol optical depth over remote oceanic regions can provide an important reference point for estimating the influence of anthropogenic aerosols on climate and climate change. The strategy considered in that paper underscores the importance of achieving a comprehensive understanding of the variation of atmospheric optical parameters in an oceanic environment.

The main goal of the current work was to study the effect of various types of air masses on the optical properties (aerosol

[1] Now at Scientific Laboratory "Tavrida" (c/o Hydrometeorological Institute), St. Petersburg, Russia.

Paper number 95JD01265.
0148-0227/95/95JD-01265$05.00

Table 1. Aerosol Optical Depth Over the Oceans and Synoptic Air Mass Types

Reference	Air Mass Type	Area	N	τ_a (550 nm)	σ	a	σ_α
Von Hoyningen-Huene and Raabe [1987]	continental	English channel, Atlantic Ocean	3	0.45	0.11		
	maritime polar	Skagerrak	2	0.07			
	maritime tropical	North Sea, Atlantic Ocean	2	0.13			
Weller and Leiterer [1988]	continental	Baltic Sea	1	0.62			
	maritime		1	0.18			
Hoppel et al. [1990, Figures 32-33]	continental air from east coast of the Unated States	Atlantic Ocean 30°N, 70°W	2	0.13		1.65	
	maritime air (subtropical high)	Atlantic Ocean 20°-25°N, 40°-55°W	3	0.08		0.95	
	remote Atlantic air	Atlantic Ocean 20°-30°N, 20°-70°W	7	0.13		0.84	
Reddy et al. [1990]	North American air	Atlantic Ocean 37°-45°N, 45°-70°W	7	0.50	0.16	1.15	0.06
	Atlantic air	Atlantic Ocean 30°-40°N, 55°-70°W	6	0.15	0.01	1.00	0.20
	Saharan air	Atlantic Ocean 15°-20°N, 35°W	2	0.38	0.06	0.37	0.09
Gulyaev et al. [1990]	maritime arctic	North Sea	1	0.15		0.94	
	continental polar	Baltic Sea	1	0.18		0.90	
		Mediterranean Sea	3	0.30	0.15	0.94	0.35
		Pacific Ocean	1	0.09		0.97	
	continental tropical	Atlantic Ocean	3	0.30	0.08	0.84	0.12
		Mediterranean Sea (June 1983)	6	0.22	0.07	0.76	0.28
		Mediterranean Sea (August-September 1986)	43	0.19	0.09	1.18	0.30
	maritime tropical	Pacific Ocean	21	0.07	0.03	0.24	0.25
		Indian Ocean, South China Sea	7	0.19	0.03	0.51	0.30
Smirnov and Gulyaw [1990]	continental polar	Atlantic Ocean 35°-40°N, 5°-20°W	3	0.14	0.09	0.92	0.15
	continental tropical		6	0.20	0.07	0.52	0.24
	maritime polar		2	0.13		0.20	
	maritime tropical		2	0.25		0.50	
Von Hoyningen-Huene and Wendisch [1994]	continental polar	Baltic Sea coat, Zingst, Germany		0.21		1.17	
	continental polar (aged)			0.20		1.06	
	continental tropical			0.29		1.12	
	continental tropical (aged)			0.24		0.92	
	maritime tropical			0.10		0.42	
	maritime polar			0.11		0.46	

N, number of analyzed spectra; τ_a(550 nm), mean value of aerosol optical depth at a wavelength 550 nm; σ, standard deviation of the aerosol optical depth; a, Angstrom parameter; σ_α, standard deviation of the Angstrom parameter.

optical depth and Angstrom parameter) of a cloudless maritime atmosphere. An analysis of the influence of meteorological parameters on atmospheric optical characteristics within a given air mass type is presented as well as a brief investigation into the applicability of well-known atmospheric optical models to the results obtained.

Instrumentation, Data Sampling, and Air Mass Characterization

The aerosol optical depth data employed in the analysis below were obtained over the Baltic Sea and North Atlantic (May-July 1984) *[Villevalde et al.,* 19891, in the Pacific Ocean (December 1988-February 1989), and in the North Atlantic (May 1989) *[Villevalde et al.,* 1994]. Another data set for the North Atlantic (May-July 1988) was previously presented by *Wolgin et d.* [1991].

The type of visible/near infrared sunphotometer employed in all these oceanic campaigns was a silicon photodiode based device which acquired solar data in eight channels ranging from 461 to 1016 nm. A second type of near infrared/short wave infrared sunphotometer employed a germanium based detector to acquire data across three channels ranging from 1016 to 1640 nm. A common channel at 1016 nm served as a redundancy check between the two types of sunphotometers. The bandwidths of the interference filters employed in these sunphotometers varied from 4 to 16 nm with a blocking factor of less than 10^{-4} outside the filter bands. The instruments were specifically designed for hand-held operation aboard an ocean-going vessel. Their viewing angle of 3 degrees permitted reliable tracking of the Sun without a significant enhancement of the signal due to near-Sun scattering *[Box and Deepuk,* 19791.

The sunphotometers were precalibrated at a high-altitude observatory (Cheget, Caucasus, Russia). The calibration constants derived from the Langley plot procedure yields errors in optical depth which do not exceed ±0.01 *[Wolgin et al.,* 1991; *Villevalde et al.,* 1994]. Rayleigh optical depths were computed according to *Elterman* [1968]. The ozone optical depth was estimated by employing simultaneous measurements of the ozone column amount and tabulated absorption coefficients [*Vigroux,* 19531. NO_2 absorption was considered negligible for the wavelengths employed in this study *[Dutton et d.,* 19941. We note that aerosol optical depths reported by *Villevalde et al.* [1989] and *Wolgin et al.* [1991] were additionally corrected for absorption by water vapor and C02 using the subarctic and midlatitude summer models of LOWTRAN-7 [*Kneizys et al.,* 19881.

Our air mass analysis followed the classical scheme with two main fronts: the arctic front, dividing arctic and polar (temperate) air masses, and the polar front, dividing polar and tropical air. Each of the three air mass types thus assumed (arctic, polar, and tropical) can be further categorized as maritime or continental according to source and trajectory information. Type and origin of the air masses were identified in the same way as it was reported by *O'Dowd et al.* [1993], using ship weather records and surface hemispheric charts provided by the National Climatic Data Center. Maps compiled for 0600 and 1800 UT on each day of observation were used. When necessary, atmospheric patterns were interpolated between them. These charts provide a general circulation pattern overview which is sufficient for air mass analysis over the ocean surface. Atmospheric fronts traced on them permit identification of air mass type according to the simple classification scheme adopted in this study. Arctic, polar, and tropical masses were identified according to the position of main fronts during the period of observation. The maritime or continental origin characterization was estimated from the circulation pattern on these surface charts. We have found that this approach is an acceptable substitute for 2 to 3 day back trajectory models when applied to optical measurement interpretation [*Smirnov et al.,* 1994]. Barometric patterns and front positions are the principal indicators when an analysis of small-scale maps is performed, but wind arrows at weather stations and temperature values were often helpful for detection of minor circulation features that were not reflected in the general pattern. We have also taken into account presence of high clouds and reported precipitation as such phenomena could explain some peculiar optical data. Table 2 gives the details of the cruises and the assignment of synoptical air mass types.

During the measurement period in the Northern Pacific from December 1988 to February 1989, the ship was moving south from latitude 40°N (December 17, 1988) to the equator (February 2, 1989) at longitudes varying between 130' and 180°E (data were taken in the southern hemisphere as well, but no weather maps were available to us for the Southern Pacific). The northern part of the cruise at latitudes higher than 18°N (January 15, 1989) was within the westerlies zone where frequent depressions with the associated atmospheric fronts advance from the Far East toward Alaska. Fast-moving cold air in cyclones arriving from the Kamchatka Peninsula or Japan was identified as continental polar as it reaches the observation point from the coast within 2-3 days and causes in the process temperature drops by as much as 10°C. Air arriving from the Philippine Sea in warm sectors of cyclones is considered maritime (polar or tropical) as it has been moving over the ocean surface for more than 3-4 days by the time that the optical measurements are acquired. At latitudes between 18°N and the equator the ship entered the trade winds belt where weak and steady northeastern winds form a quasi-constant circulation pattern. No atmospheric fronts are present as we approach the equator; this air can be considered "true maritime tropical" with temperatures in the 25-30°C range. Figure 1 gives examples of surface weather charts for Pacific Ocean.

Three data sets from the North Atlantic acquired in 1984, 1988, and 1989 have been analyzed. Very dynamic atmospheric patterns typical for this area are summarized by *O'Dowd et al.* [1993]. The area is mostly dominated by maritime polar air advancing from the northwest Atlantic or mid-Atlantic. Some of these masses pass over Ireland and Great Britain and form modified maritime air type. Advections of maritime arctic air via the Norwegian Sea or Greenland are frequent in the rear parts of depressions. Air passing over the snow-covered surface of Greenland is still considered maritime. Continental polar air reaches the area from the east or southeast if a high-pressure zone (often an extension of the Siberian anticyclone) is present over Europe. Figure 2 gives examples of surface weather charts for the North Atlantic.

The first data set was taken between May 14 and July 7, 1984, in the Baltic and Norwegian Seas in highly variable conditions [*Villevalde et al.,* 19891. On 4 out of 10 days an anticyclonic pattern caused advection of continental polar air from Eastern and Central Europe. Only three occurrences of true maritime (arctic) air were identified, the remaining one being a

Table 2. Detailed (Half Day) Characterization of Synoptical Air Mass Types for the Cruise Data Summarized in Table 3

Date	Latitude	Longitude	Air Mass Type
Baltic Sea and North Atlantic, 1984 [Villevalde et al., 1989]			
May 14, 1984-1	59.5°N	23.0°E	hp
May 14, 1984-2	59.2°N	23.2°E	hp
May 16, 1984-2	56.1°N	19.1°E	cP
May 18, 1984-2	56.1°N	11.8°E	mmP
May 20, 1984-2	60.5°N	4.1°W	cP
May 26, 1984-2	65.0°N	2.7°W	mA
June 5, 1984-2	62.3°N	4.4°W	cP
June 6, 1984-1	62.6°N	4.8°W	cP
June 25, 1984-2	63.5°N	1.5°W	mA
July 6, 1984-2	59.0°N	21.1°E	mA
July 7, 1984-1	59.3°N	23.5°E	hp
North Atlantic, 1988 [Wolgin et al., 19911			
May 23, 1988-1	62.6°N	4.7°E	cP
May 23, 1988-2	63.0°N	3.1°E	cP
May 24, 1988-1	63.0°N	3.1°W	cP
May 24, 1988-2	63.0°N	3.3°W	cP
May 26, 1988-2	64.0°N	3.0°W	cP
June 8, 1988-2	73.7°N	2.0°W	mA
June 19, 1988-1	67.1°N	0.4°W	mP
July 3, 1988-2	68.8°N	2.0°W	mA
North Atlantic, 1989 [Villevalde et al., 1994]			
May 14, 1989-2	58.0°N	6.3°E	mmP
May 19, 1989-1	64.0°N	5.5°E	mA
May 20, 1989-1	65.0°N	5.2°E	mA
May 23, 1989-1	66.0°N	2.7°E	mmP
May 23, 1989-2	66.0°N	7.0°E	mmP
May 26, 1989-2	67.3°N	6.2°W	mA
Pacific Ocean, 1988-1989 [Villevalde et al., 1994]			
Dec. 17, 1988-1	40.0°N	170.0°E	cP
Dec. 17, 1988-2	39.4°N	170.0°E	cP
Dec. 20, 1988-1	30.0°N	173.1°E	mP
Dec. 21, 1988-2	30.0°N	180.0°E	mP
Dec. 22, 1988-1	26.4°N	180.0°E	mP
Dec. 22, 1988-2	25.0°N	180.0°E	cP
Dec. 23, 1988-2	27.4°N	174.2°E	cP
Dec. 25, 1988-1	30.0°N	164.7°E	cP
Dec. 27, 1988-1	30.0°N	155.1°E	cP
Dec. 27, 1988-2	30.0°N	154.7°E	cP
Jan. 13, 1989-1	22.4°N	133.8°E	cP
Jan. 13, 1989-2	21.8°N	135.0°E	cP
Jan. 14, 1989-1	20.2°N	139.2°E	mP
Jan. 14, 1989-2	19.9°N	139.9°E	mP
Jan. 15, 1989-1	18.2°N	143.7°E	mT
Jan. 15,1989-2	18.0°N	144.3°E	mT
Jan. 16,1989-1	16.2°N	147.5°E	mT
Jan. 16, 1989-2	16.1°N	148.0°E	mT
Jan. 17, 1989-1	14.2°N	151.6°E	mT
Jan. 17, 1989-2	13.6°N	152.8°E	mT
Jan. 18, 1989-1	11.2°N	155.8°E	mT
Jan. 18, 1989-2	10.8°N	156.2°E	mT
Jan. 23, 1989-1	3.2°N	174.9°E	mT
Jan. 23, 1989-2	3.5°N	176.5°E	mT
Jan. 25, 1989-1	7.9°N	180.0°E	mT
Jan. 25, 1989-2	9.2°N	180.0°E	mT
Jan. 26, 1989-1	13.0°N	180.0°E	mT
Jan. 26, 1989-2	14.2°N	180.0°E	mT
Jna. 27, 1989-1	17.4°N	180.0°E	mT
Jan. 27, 1989-2	18.4°N	180.0°E	mT
Jan. 20, 1989-1	13.5°N	180.0°E	mT
Jan. 30,1989-2	12.3°N	180.0°E	mT
Jan. 31, 1989-2	8.6°N	180.0°E	mT
Feb. 1, 1989-2	4.9°N	180.0°E	mT
Feb. 2, 1989-1	2.3°N	180.0°E	mT
Feb. 2, 1989-2	0.8°N	180.0°E	mT

The numbers after the dates of measurements indicate (1) before noon and (2) afternoon averages. Abbreviations for air mass type: hp, high pressure; cP, continental polar; mmP, modified maritime polar; mA, maritime arctic; mT, maritime tropical.

modified maritime air, probably reaching the Baltic Sea via Scandinavia. The next data set was obtained between May 23 and July 3, 1988, in the middle of the Norwegian Sea [*Wolgin et al.*, 1991]. Some measurements were taken in maritime air moving along a depression from Greenland (arctic) or mid-Atlantic (polar). On 3 days air that had been passing over the European coast at the southeastern edge of the Atlantic cyclones was observed. The third set was taken on May 14 - May 26, 1989, in the Norwegian Sea [Villevalde et al., 1994]. Depressions following a low-pressure trough across the North Atlantic formed a steady zonal circulation pattern for the whole period of observations. Arctic and polar maritime air (modified) was dominant. No continental air masses occurred during this period.

We estimate that the combination of these three data sets is sufficient for the characterization of the four main air mass types common in the North Atlantic (maritime polar, maritime arctic, modified maritime polar, and continental polar). On the other hand, air mass types with rare occurrence in this area, namely, the continental arctic and any tropical air, are not presented in the analysis.

Thirty six half-day measurement averages (where each average is taken over measurements acquired before noon or measurements acquired in the afternoon) were considered for the Pacific data set while 25 such averages were computed for the Baltic Sea and North Atlantic data. We deliberately employed half-day averages in order not to overestimate the statistical weight of air masses whose importance would be biased by a large number of optical measurements being made during a particular half-day period.

Results

Optical Statistics Referenced to Synoptic Air Mass

Because the standard deviations were not included in a significant number of the data sources considered in Table 1, we could not comprehensively evaluate the variability of τ_a and α for various air mass types. Nevertheless, one can observe that the most extreme optical variability occurs for continental polar (cP) air masses. This high degree of variability is largely attributable to the diverse contributions of a variety of continental aerosol sources. The enrichment of continental air by maritime aerosol ("stationary" and "fresh" components, as per *Kneizys et al.* [1988]) is an additional source of variability which depends upon the trajectory time above the ocean. This latter effect leads to smaller Angstrom parameter values as a consequence of the presence of larger particles (radius larger than 0.5 μm [*Hoppel et al.*, 19901) in the aerosol size distribution.

Table 3 summarizes measurements of aerosol optical depth in oceanic areas for which air mass type analyses have been performed in the current study. One can observe indications of differences between continental and maritime air masses in terms of the aerosol optical depth value as well as the Angstrom parameter. The latter was calculated in the 460-1016 nm range in order to provide a common basis for comparison with previous results. As would be expected, the continental polar air mass type is, as a rule, more turbid than maritime types. Also it can be noted that the spectral behavior of $\tau_a(\lambda)$ is more selective in continental air masses (higher Angstrom parameter value corresponding to generally smaller particles). Smaller mean α values of continental polar air mass in the

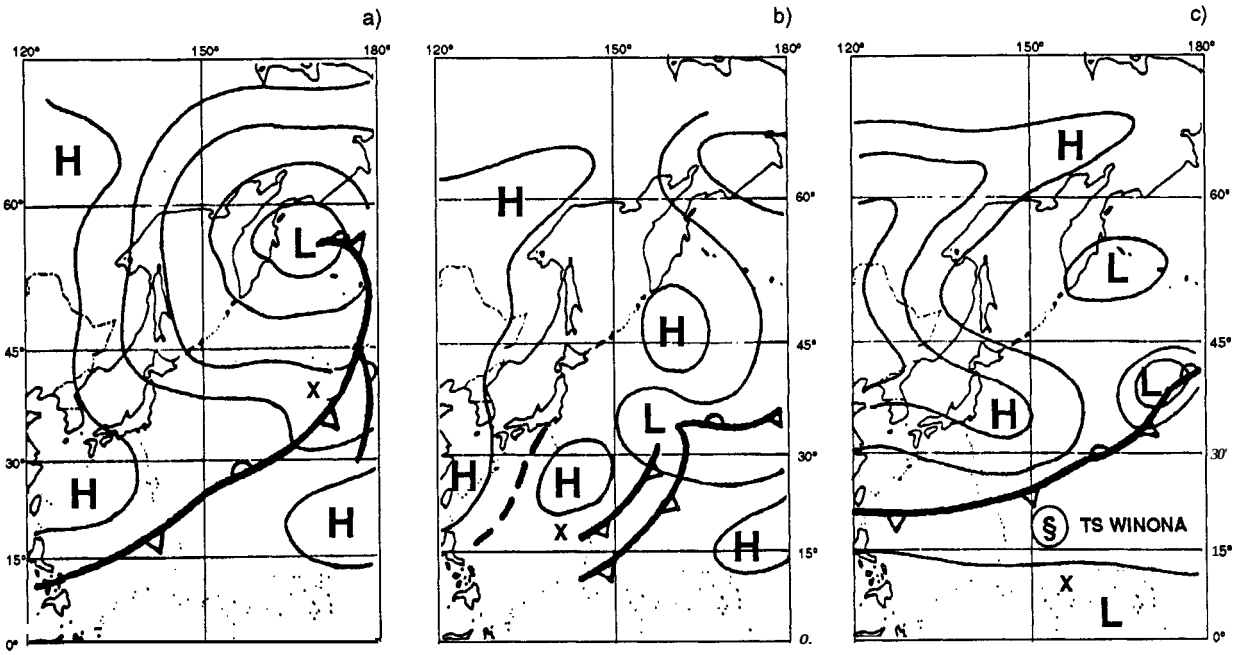

Figure 1. Examples of surface weather charts for Pacific Ocean. Cross indicates the vessel position: (a) continental polar air on December 17, 1988; (b) maritime polar air on January 14, 1989; (c) maritime tropical air on January 18, 1989.

Pacific Ocean as compared to the North Atlantic may be attributed, in the first instance, to different routes and to the different degree of aerosol contamination and deposition along the way.

Figure 3a shows the mean aerosol optical depth spectra in various air mass types over the Pacific Ocean as derived from our data set. In spite of the small number of half-day averages the maritime polar (mP), cP, and maritime tropical (mT) data sets are statistically distinguishable (at the 95% confidence level) either in terms of τ_a or in terms of α.

From Figures 3b and 3d-3f and Table 3 one can observe that the mean values of τ_a and α for maritime arctic (mA) air masses coincide well. Moreover, these results are close to those obtained by *Smirnov et al.* [1994] for mA masses over continental sites (0.10±0.03 and 0.90±0.38 respectively). These latter findings indicate that the optical properties of the maritime arctic air mass can be described in a more general sense and that even in the case of a perturbing continental trajectory the air mass tends to preserve optical properties.

Three half-day measurement averages in the Baltic Sea were obtained in continental polar air conditions but in the center of strong anticyclone. The mean values of τ_a and α (0.12 and 0.77 correspondingly) are close to the results of *Hoppel et al.* [1990] for remote Atlantic air and also to the values obtained in the Pacific Ocean for maritime polar air (Table 3). At the same time the synoptic situation in the Baltic Sea could not be considered as maritime polar. Owing to the lack of data we simply categorized the results as having been acquired in the center of the high-pressure (hp) system (Figure 3c).

We would like to point out the differences in optical properties observed for the modified maritime polar (mmP) air mass in the North Atlantic (1989) and Baltic Sea (1984) data sets (Figures 3c and 3f). In these cases the Angstrom parameter values are practically the same, but τ_a differs by a factor of 5. Our synoptical analysis made for the Baltic Sea measurement (we have a single half-day average in such conditions) demonstrated that the source of this optically turbid air mass could not be identified as continental. Such high turbidity was associated with strong contamination of maritime air during its passage over the British Isles and Western Europe. In spite of this contamination we still considered the air mass, by virtue of its origin, to be of the modified maritime type.

Frequency of occurrence distributions for τ_a and α are presented for the Pacific Ocean in Figures 4a and 4b and for the Baltic Sea and North Atlantic in Figures 4c and 4d. In Figure 4 we can observe significant aerosol spectral selectivity (high $\alpha \cong 0.9$-1.3 or correspondingly small average particle size) in cP air (Figures 4b and 4d) and relatively neutral (modal value of $\alpha \sim 0.5$) spectral dependency (large average particle sizes) in mT air masses (Figure 4b). A narrow frequency distribution of α and τ_a is evident for mA air masses (Figures 4c and 4d).

Table 4 is a summary of the results for the different cruises of Table 3 as a function of overall air mass statistics. Our approach in the synoptical analysis of the optical data is to, first, investigate the differences between mean aerosol optical depths (as an indicator of mean columnar number density), and then, if the differences are not significant, in terms of the mean Angstrom parameter (as a mean indicator of the average particle size). This strategy was inspired by previous results on the generally greater information content (variance) of τ_a versus α [*Volgin et al.*, 19881.

Note that the results of our analysis are not inconsistect with those presented in Table 1. Variations in the optical properties of continental polar air masses are quite understandable given the variety of aerosol sources and differences in air mass history. The mean Angstrom parameter computed for maritime arctic air (Table 4) is comparable with the single measurement presented in Table 1, while the aerosol optical depth is smaller. Mean aerosol optical depths and Angstrom parameters of maritime polar and maritime tropical

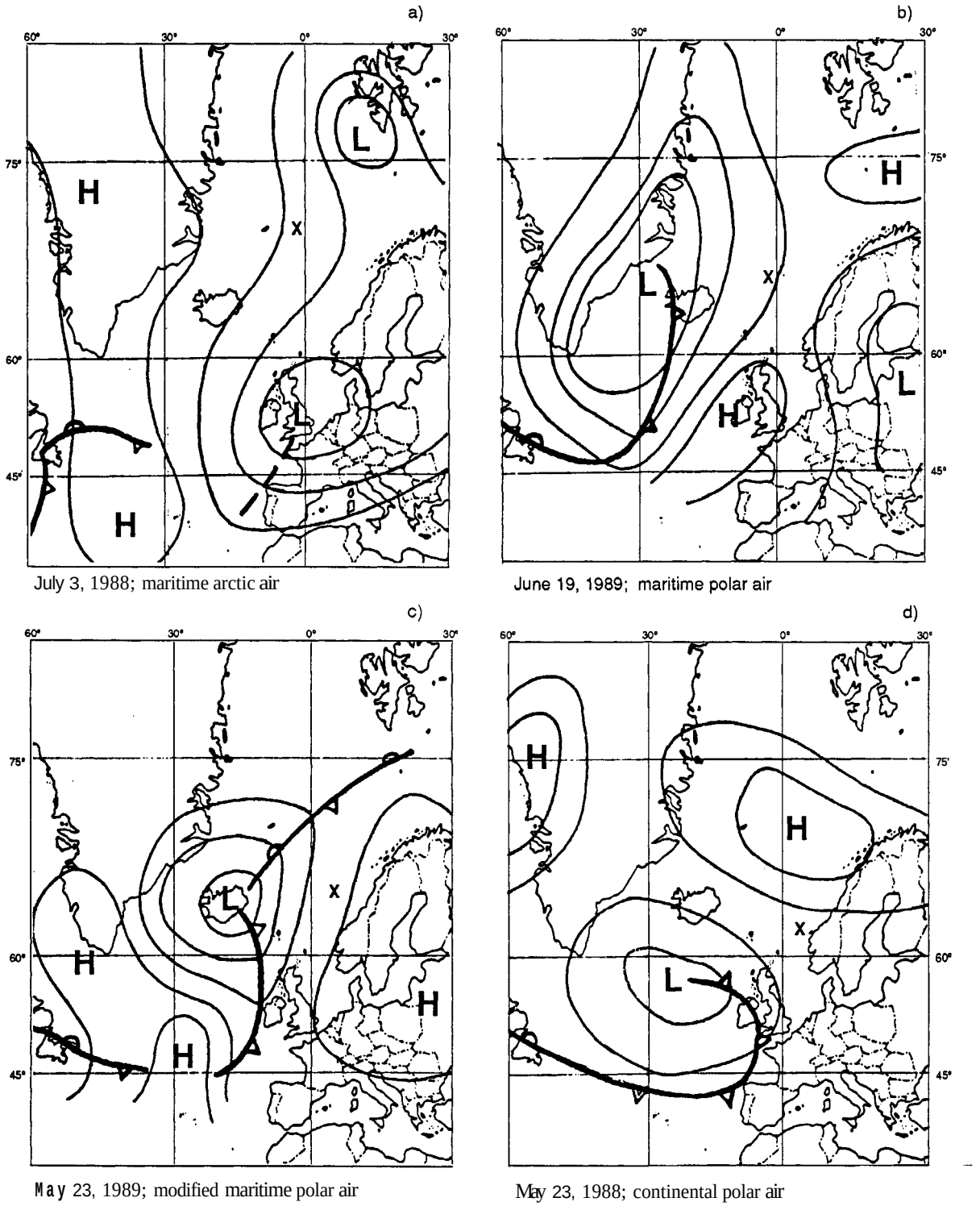

Figure 2. Examples of surface weather charts for the North Atlantic. Cross indicates the vessel position: (a) maritime arctic air on July **3, 1988;** (b) maritime polar air on June **19, 1988;** (c) modified maritime polar air on May **23, 1989;** (d) continental polar air on May **23, 1988.**

air from Table **1** correspond well to the mean values obtained in the current work.

Values of τ_a **(550** nm) obtained by ***Reddy et al.*** [1990] for those days on which he states that the air mass type was primarily maritime tropical (not listed in the summary statistics of Table 1) agree with the value of aerosol optical depth given in Table **4** within 1 standard deviation. This is not, however, true for the Angstrom parameter ***a*** values. ***Reddy et al.*** [1990] noted that the values of τ_a at 500 nm were below **0.20** and that ***a*** (based on four wavelengths in the range 380-**778** nm) varied from 0.55 to **1.36** in essentially maritime tropical air masses. However, he did cast doubt on the high α

Table 3. Aerosol Optical Depths and Synoptic Air Mass Types for the Current Work

Air Mass Type	Area	N	τ_a (550 nm)	σ	α	σ_α
Continental polar	Pacific Ocean	9	0.12	0.04	0.82	0.14
	Baltic Sea (May, July 1984)	1	*0.46*		1.14	
	North Atlantic (May-June 1984)	3	0.23	0.04	1.33	0.04
	North Atlantic (May-July 1988)	5	0.15	0.04	1.24	0.15
Maritime arctic	Baltic Sea (May, July 1984)	1	0.09		0.99	
	North Atlantic (May-June 1984)	2	0.09		0.99	
	North Atlantic (May-July 1988)	2	0.06		0.90	
	North Atlantic (May 1989)	3	0.10	0.01	0.98	0.28
Maritime polar	Pacific Ocean	5	0.09	0.004	*0.52*	0.35
	North Atlantic (May-July 1988)	1	0.16		0.11	
Maritime tropical	Pacific Ocean	22	0.15	0.04	0.42	0.23
Maritime polar (modified)	Baltic Sea (May, July 1984)	1	0.45		1.37	
Center of a high-pressure system	Baltic Sea (May, July 1984)	3	0.12	0.04	0.77	0.10
Maritime polar (modified)	North Atlantic (May 1989)	3	*0.09*	0.03	1.23	0.11

N, number of analyzed spectra; τ_a(550 nm), mean value of aerosol optical depth at a wavelength 550 nm; σ, standard deviation of the aerosol optical depth; α, Angstrom parameter; σ_α, standard deviation of the Angstrom parameter.

values obtained by comparing these to estimates of 0.2-0.4 for maritime air (estimations made by *Von Hoyningen-Huene and Raabe* [1987]). They attributed this shift to the differences in the wavelength range where measurements were made.

Wind Speed and Relative Humidity: Optical Correlations in the Light of Air Mass Constraints

The effect of wind speed (v) on the concentration and size distribution of sea-salt aerosol was comprehensively and successfully studied during the last four decades (see summary by *Fitzgerald* [1991]). In contrast, the influence of wind speed on aerosol optical depth in the whole atmospheric column is a much more difficult problem. In spite of the evident link between optical turbidity and wind particle generation, it is not easy to detect the effect of local sea-spray aerosol on $\tau_a(\lambda)$, since it is masked by the background aerosol. Accordingly, aerosol surface generation effects can only be inferred on the $\tau_a(\lambda)$ curve when measurements are taken in a reasonably transparent atmosphere. An important additional condition is that a relationship between τ_a and wind speed needs to be ascertained in the same air mass type in order to minimize the influence of other meteorological parameters on τ_a. The clearest evidence of the correlation between wind speed and aerosol optical depth should be obtained when all other meteorological parameters are simply the same over the range of wind speeds considered.

The data reported by *Hoppel et al.* [1990] indicate that the deck level measured scattering coefficients have a stronger dependence on wind speed at infrared wavelengths than at visible wavelengths. In order to eliminate the effect of relative humidity on the variability of the scattering coefficient, *Hoppel et al.* [1990] normalized their measured values to a relative humidity of 75%. They pointed out that there was considerable scatter in the data despite the removal of relative humidity effects and that this scatter could at least, in part, be attributable to variations in air mass history. These findings indicate the relevance of investigating, as we did, the relationship between τ_a and wind speed in the same air mass type.

One can observe in Figures 5a and 5b the regression of aerosol optical depth at a wavelength of 1640 nm and the Angstrom parameter versus wind speed in a maritime tropical air mass. This data set which corresponds to the last entry of Table 4 (Pacific Ocean) was the only maritime data set with a statistically acceptable number of measurements. The correlation coefficient between τ_a (1640 nm) and wind speed is equal to 0.60, while the correlation coefficient for the total Pacific Ocean data set (reported by *Villevalde et al.* [1994]) was equal to 0.38. This means that reducing the number of measurements increased the correlation coefficient since the remaining data were effectively characterized by more uniform atmospheric conditions. In addition, a statistically significant negative correlation (-0.57) between α and v gives further indirect evidence of the effects of wind on the aerosol size

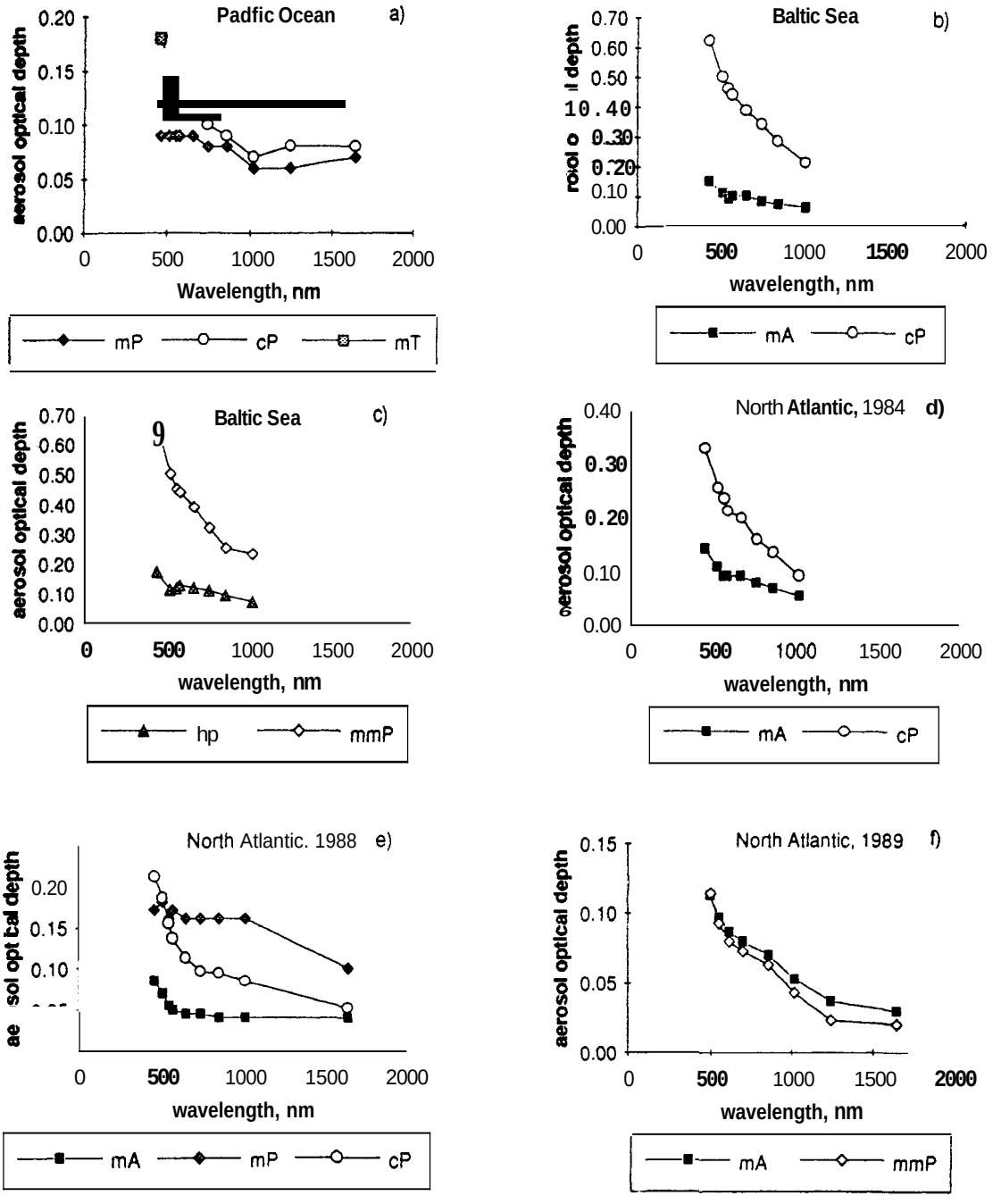

Figure 3. Mean aerosol optical depth spectra in various air masses. The air mass codes are mA, maritime arctic; cP, continental polar: mP, maritime polar; mmP, modified maritime polar: mT, maritime tropical; hp, high pressure system.

distribution. The wind-driven contribution of large sea-spray particles to the measured particle number was clearly demonstrated by *O'Dowd et al.* [1993].

The slopes calculated for our regression for τ_a (1640 nm) versus v (0.007 s/m) and that reported by ***Platt and Patterson*** [1986] for a wavelength of 500 nm (0.003 s/m) are remarkably coherent. We consider this agreement to be about as good as can be expected since Platt's results were obtained for a different (and less than optimal) wavelength and since they were obtained for a somewhat different environment (on the coast at a height of 94 m above sea level). His measurements at the 94-m height permitted the monitoring of principally the "stationary" component *[Kneizys et al.*, 1988] of the maritime aerosol. Our measurements showed a stronger dependence (higher regression slope for aerosol optical depth versus wind speed) due to the greater sensitivity of the infrared channel and the greater contribution of the "fresh" aerosol component [*Kneizys ef al.,* 1988] to the total concentration at the deck level height (the "fresh" component being more sensitive to the current wind speed). Thus we were able to detect with confidence the effect of local sea-spray aerosol on $\tau_a(\lambda)$.

Interesting results were obtained with regard to the effect of deck level relative humidity on aerosol optical depth. Figures 6a and 6b are plots of aerosol optical depth at a wavelength of

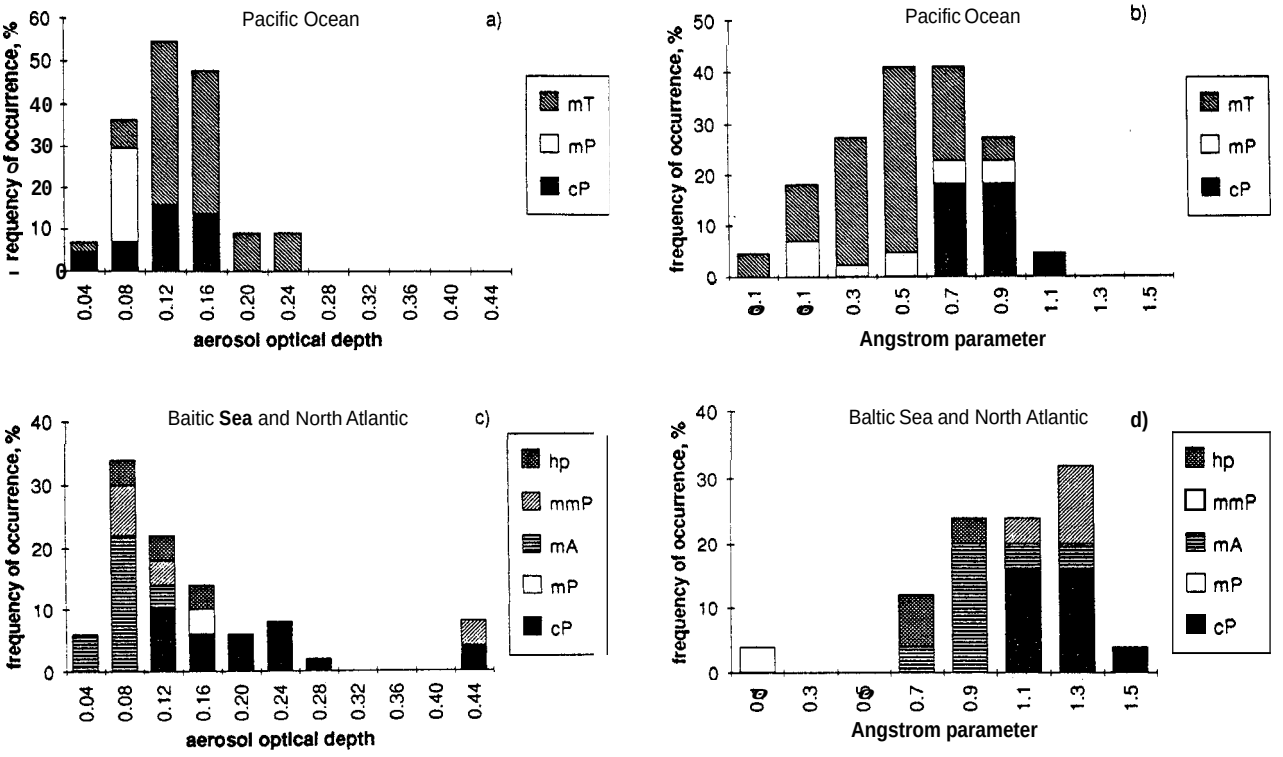

Figure 4. Frequency of occurrence of aerosol optical depth at a wavelength 550 nm and Angstrom parameter in various air masses. See Figure 3 for the air mass codes.

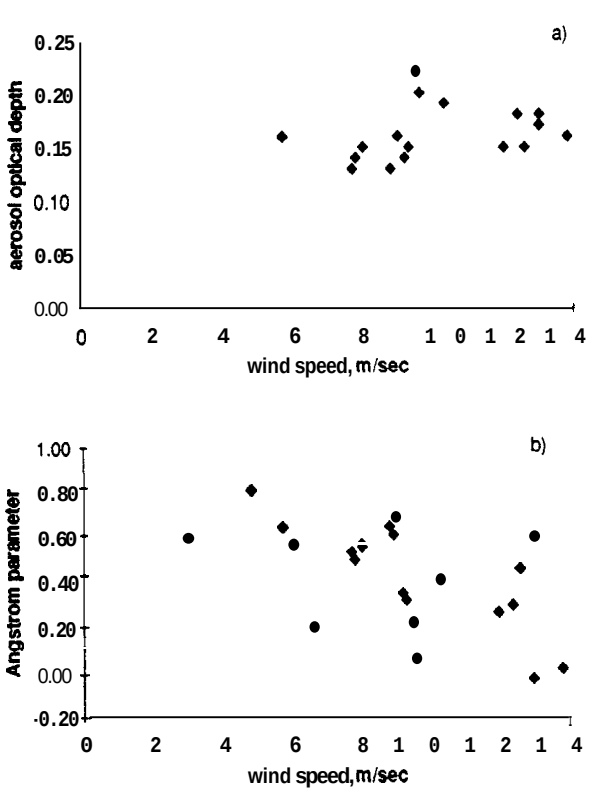

Figure 5. (a) Plot **of** aerosol optical depth at a wavelength **1640** nm and **(b)** Angstrom parameter versus wind speed measured at deck level in maritime tropical air **mass.**

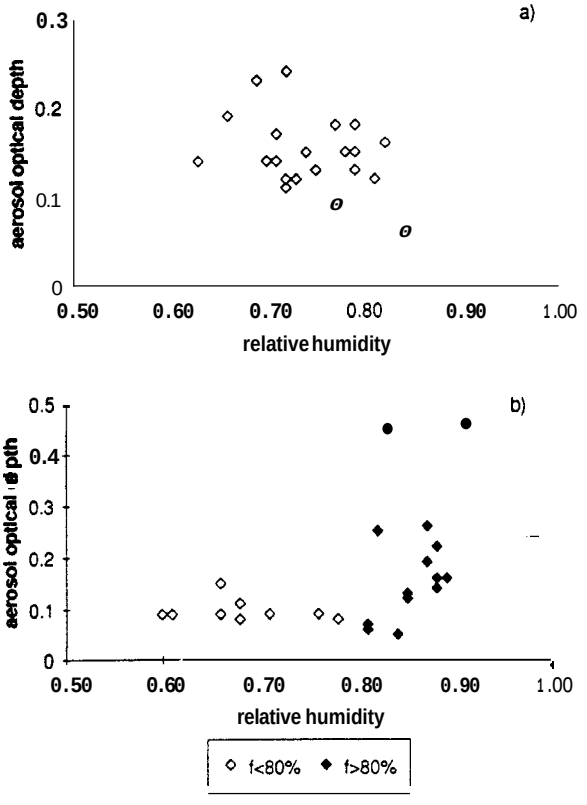

Figure 6. Plot of aerosol optical depth at a wavelength 550 nm versus relative humidity measured at deck level. (a) Maritime tropical air mass in Pacific Ocean, and (b) all data set obtained in the Baltic Sea and North Atlantic.

Table 4. Air Mass Types Statistically Distinguishable in Terms of the Structure of $\tau_a(\lambda)$

Air Mass Type	Area	N	τ_a (550 nm)	σ	a	σ_α
Continental polar	Pacific Ocean	9	0.12	0.04	0.82	0.14
	North Atlantic	8	0.18	0.06	1.27	0.14
Maritime arctic	North Atlantic	7	0.08	0.02	0.96	0.19
Maritime polar	Pacific Ocean	5	0.09	0.004	0.52	0.35
Maritime polar (modified)	North Atlantic	3	0.09	0.03	1.23	0.11
Maritime tropical	Pacific Ocean	22	0.15	0.04	0.42	0.23

N, number of analyzed spectra; τ_a(550 nm), mean value of aerosol optical depth at a wavelength 550 nm; σ, standard deviation of the aerosol optical depth; a, Angstrom parameter; σ_α, standard deviation of the Angstrom parameter.

550 nm versus relative humidity. We plotted the data for maritime tropical air mass in Figure 6a and all the data set obtained in the Baltic Sea and North Atlantic in Figure 6b.

Smimov and Shifrin [1989] reported a lack of correlation between measurements of aerosol optical depth and relative air humidity f acquired synchronously at deck level. In the "dry" (f<75%) and the "moist" (f>75%) data sets, respectively, anticorrelation and correlation between τ_a and f were observed. Anticorrelation was explained by the fact that an increase in turbulent exchange on the one hand leads to a decrease in f and in turn to an increase in τ_a as a result of increased transfer of droplets from the sea surface into the atmosphere. This phenomenon was observed for the "dry" data set for which the surface attenuation coefficient is known to be almost independent of humidity [*Shettle* and *Fenn*, 19791, while positive correlation was observed for the "moist" data set for which the rapid increase of attenuation coefficients with f dominated the effects associated with turbulent exchange.

Figure 6 supports the arguments for the above-mentioned trend in terms of the τ_a versus f dependency. In the Pacific Ocean we obtained negative correlation (-0.38) between τ_a and f for maritime tropical air mass (statistically significant value at the 95% level is -0.40). It should be noted that there are several points in Figure 6a between 75 and 85% and yet there is no obvious increase in τ_a with increasing f. We can only presume that the turbulent exchange effect offset the particle growth for those relative humidities which actually exceed the deliquescence points of the water soluble aerosols in this environment (76% for sodium chloride and 82% for ammonium sulfate as the two most pertinent examples). The same type of aerosol optical depth trend cannot be excluded as a possibility in the case of Figure 6b but unfortunately is not statistically significant at relative humidities f<80% (correlation coefficient of -0.22). However, when the relative humidity surpasses the deliquescence point of the aerosols (i.e., in the neighborhood of 80%), condensational processes lead to an increase in τ_a with increasing f. This trend can be seen in Figure 6b although the correlation coefficient of 0.37 was not significant at the 95% level (the statistically significant value at the 95% level is 0.5).

Analysis of Aerosol Optical Depth Spectra in Various Air Mass Types

To interpret the mean aerosol optical depth spectra in various air mass types it is evident that at least in the first instance we should employ established and well-known aerosol parameterization models. These models which are functions of bimodal and trimodal size distributions are used to simulate optical depth spectra which are iteratively compared to the measured spectra until a satisfactory match is achieved. As a criteria of fit we assumed that the measured and calculated spectra should not differ by more than ±0.01 (measurement error) in each channel. This criteria is more conservative than a simple 0.01 constraint on the rms error. For our simulations the models of the World Climate Programme (WCP) [*McClatchey et al.*, 19831 and Navy Maritime model in LOWTRAN-7 code [*Kneizys et al.*, 19881 were used.

To illustrate the applicability of the Navy Maritime aerosol model to the statistically sparse results obtained in the North Atlantic, we merged three half-day averages measured in 1984 and five from the paper of *Wolgin et al.* [1991] into one cP class data ensemble. In addition, we created a joint mA data set which incorporates two half-day averages from the 1984 results, three from the 1989 results and two averages reported by *Wolgin et al.* [1991].

Cwing to a lack of measurements and to the complexity of the synoptical results obtained, we did not consider the data measured in the Baltic Sea. Thus only the data for the Pacific Ocean and the North Atlantic were employed.

Consider first the simulations made using the Navy Maritime aerosol model. We assumed that for all the maritime air mass types the air mass character (C) , which describes the influence on number distribution of aerosols of continental origin, is equal to unity (open ocean). In order to yield an acceptable fit to the spectra of τ_a measured in continental polar air, we took the liberty of varying the air mass character parameter to a certain extent. Using available information on wind speed during the measurement period, we averaged the wind speed data over each period to obtain the input parameter of current wind speed (v). No estimation of the 24-hour average speed (v), which defines the "stationary" component of the maritime aerosol model, could be made from the available data.

The simulation results which are shown in Figures 7a-7c, 7e, and 7f illustrate how the mean spectra satisfy the fit criteria. The LOWTRAN-7 simulations yielded an acceptable fit to the North Atlantic spectra (Figures 7e and 7f) according to the error criteria defined above. The Pacific spectra (Figures 7a-7c) were found to be inconsistent with the simulations in the short-wave infrared channels (1240 nm and 1640 nm). This disparity was a factor of 3 or 4 greater than the measurement error. In contrast, good agreement was achieved between

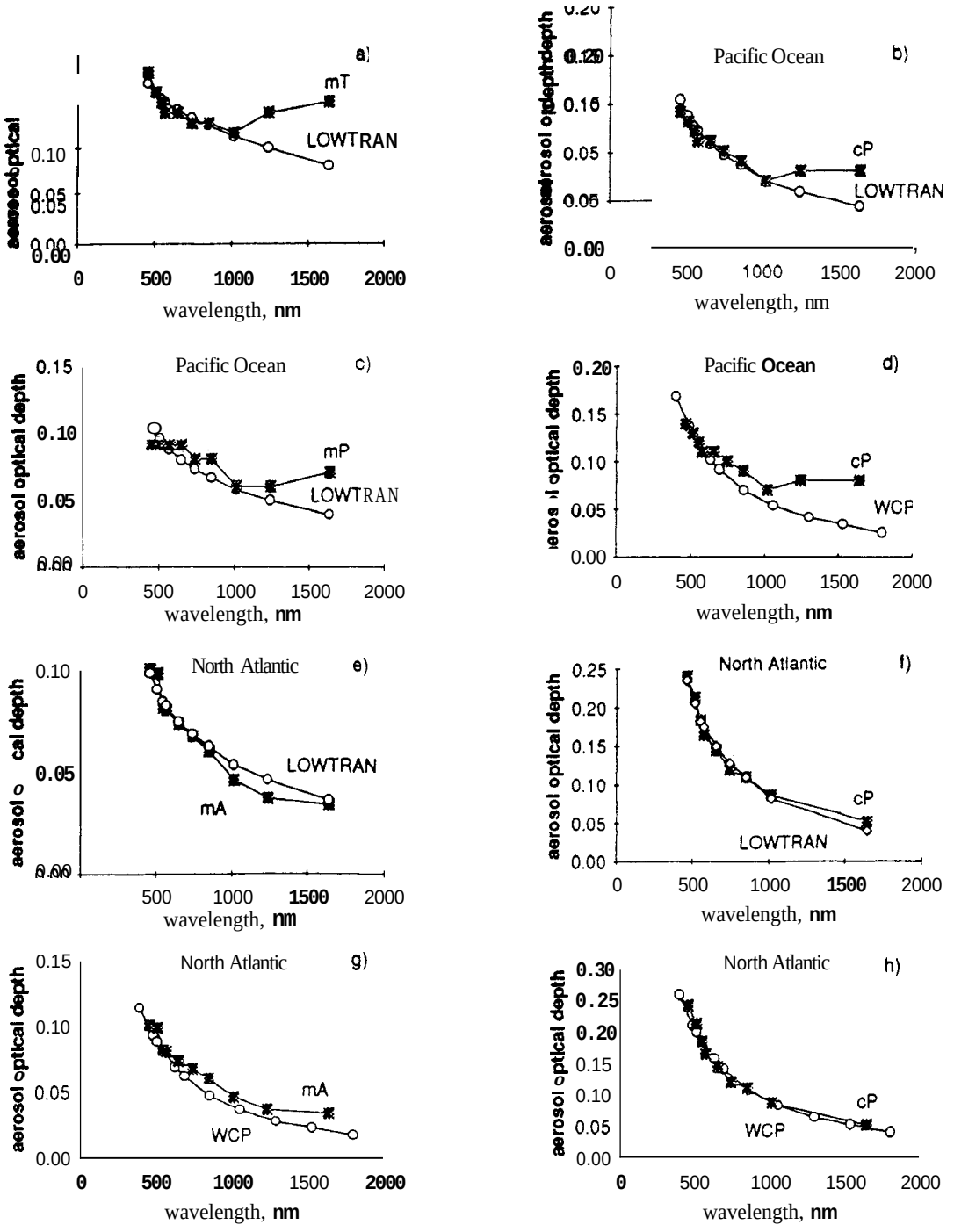

Figure 7. Comparison of measured (asterisk) and calculated (open circle) opticla depth spectra for the LOWTRAN-7 (Navy Maritime model) simulations and the WCP (continental model) simulations. Pacific Ocean: (a) mT, C=1, v =7.0 m/s, v=9.1 m/s; (b) cP, C=3, v =3.8 m/s, v=9.8 m/s; (c) mP, C=1, v =4.0 m/s, v=7.0 m/s. North Atlantic (e) mA, C=1, v =4.0 m/s, v=8.5 m/s; (f) cP, C=5, v =3.1 m/s, v=9.5 m/s. Pacific Ocean (d) cP and North Atlantic (g) mA and (h) cP. See Figure 3 for the air mass codes.

measured and calculated spectra in the visible and near infrared channels. We further note that the disagreement in the last two channels is less for continental air than for maritime. This result is consistent with the argument that the increase of aerosol optical depth in the range 1016-1640 nm, reported by *Villevalde et al.* [1994], was induced by aerosols of local origin (sea spray). The authors employed a microphysical bimodal aerosol model composed of a fine mode (Rn=0.08 μm, σ=1.7) and a narrow coarse mode (Rn=1.0 μm, σ=1.2) for which the concentrations were adjusted to achieve the fit criteria described above (Rn and σ are the geometric mean radius and exp(standard deviation) of the standard lognormal distribution). These latter fits, which duplicated the short-wave infrared channel increases seen in Figure 7, also yielded reasonable number densities for such oceanic regions.

The $\tau_a(\lambda)$ spectral functions derived from the continental WCP model for the North Atlantic data were successfully adjusted to achieve a fit criteria for the mA and cP sets (Figures 7g and 7h). The similarity between the spectral curves of the continental model and the maritime arctic air mass is reflected in the value of their Angstrom parameters, which are 1.18 and 0.96, respectively. The best fit that was achieved by the continental WCP model for the Pacific measurements is shown in Figure 7d. However, it is clear that the disparity in the blue and short-wave infrared ranges significantly exceeds 0.01. The maritime WCP model did not yield an acceptable fit to the aerosol optical depth spectra for either the Pacific or the North Atlantic data.

Conclusions

The principal conclusion from our work can be summarized as follows:

1. It was found that the optical properties (aerosol optical depth and Angstrom parameter) of continental and maritime air mass types differ significantly for the data employed in this study (see Table **4).** The limitations of data set size, however, preclude the establishment of reliable statistical characteristics for the a priori estimation of atmospheric optical properties as a function of air mass type.

2. The air mass discriminating process permitted a more rigorous analysis of the link between wind speed and aerosol optical depth variations. It was determined that τ_a for maritime tropical air masses has a significant dependence on wind speed at the 1640-nm infrared wavelength and that the observed optical variations are consistent with arguments on wind velocity and the generation of maritime aerosols. In support of the arguments for air mass analysis, the correlations of maritime tropical air mass data set were found to be significantly better than those obtained in a previous study (on a super set of the same Pacific Ocean data *[Villevalde et al.*, 19941) where no air mass discrimination was made.

3. The aerosol optical depth and relative humidity analysis was not statistically conclusive. The trends observed were nonetheless found to be consistent with the explanation put forth by ***Smirnov and Shifrin*** [1989] on the relationship between τ_a (550 nm) and deck level relative humidity f. When relative humidity is less than 75-80%, an increase in turbulent exchange leads to a decrease in f and to an increase in τ_a. In contrast, if relative humidity is high enough the rapid increase of the attenuation coefficient with f dominates effects associated with turbulent exchange.

4. Simulation of the aerosol optical depth spectra in various air mass types employing well-known standard aerosol parameterization models showed good agreement with the experimental results in the visible and near infrared range. In the short-wave infrared range the disparity between the measurements and spectra calculated from the standard aerosol models significantly exceeds the measurement error.

Acknowledgments. The authors wish to acknowledge the financial support of the Hydrometeorological Institute and the Arctic and Antarctic Scientific Research Institute, St. Petersburg, Russia, and the National Sciences and Engineering Research Council (NSERC) of Canada, the Atmospheric Environment Service (AES) of Environment Canada, and the Association of Universities and Colleges of Canada (AUCC).

References

Box, M.A., and A. Deepak, Atmospheric correction to solar radiometry, *Appl. Opt., 18,* 1941-1948, 1979.

Dutton, E.G., P. Reddy, S. Ryan, and J.J. DeLuisi, Features and effects of aerosol optical depth observed at Mauna Loa, Hawaii:1982-1992, *J. Geophys. Res., 99,* 8295-8306, 1994.

Elterman, L., UV, visible and IR attenuation for altitudes to 50 krn, *AFCRL-68-0153*, 49 pp; Air Force Cambridge Res. Labs., Hanscom AFB, Mass., 1968.

Fitzgerald, J.W., Marine aerosols: A review, *Atmos. Environ. Part A, 25,* 533-546, 1991.

Gulyaev, Y.N., O.A. Yershov, A.V. Smirnov, and K.S. Shifrin, The air masses influence on spectral transmittance in typical maritime regions (in Russian), in ***Atmospheric and Marine Oprics,*** edited by K.S. Shifrin, pp. 96-97, State Optical Institute, Leningrad, 1990.

Hoppel, W.A., J.W. Fitzgerald, G.M. Frick, R.E. Larson, and E.J. Mack, Aerosol size distributions and optical properties found in the marine boundary layer over the Atlantic Ocean, *J. Geophys. Res., 95,* 3659-3686, 1990.

Kneizys, F.X., E.P. Shettle, L.W. Abreu, G.P. Anderson, J.H. Chetwynd, W.O. Gallery, J.E.A. Selby, and S.A. Clough, Atmospheric transmittance/radiance: The LOWTRAN-7 model, ***Rep. AFGL-TR-88,*** 306 pp; *Air* Force Geophys. Lab., Bedford, Mass., 1988.

McClatchey, R.A., H.-J. Bolle, and K.Y. Kondratyev, A preliminary cloudless standard atmosphere for radiation computation, Report of the experts meeting on aerosols and their climatic effects, ***Rep. WCP-55,*** World Meteorol. Org., Geneva, 1983.

O'Dowd, C.D., M.H. Smith, and S.G. Jennings, Submicron particle, radon and soot carbon characteristics over the northeast Atlantic, *J. Geophys. Res., 98,* 1123-1135, 1993.

Penner, J.E., R.J. Charlson, J.M. Hales, N.S. Laulainen., R. Leifer, T. Novakov, J. Ogren, L.F. Radke, S.E. Schwartz, and L. Travis, Quantifying and minimizing uncertainty of climate forcing by anthropogenic aerosols, ***Bull. Am. Meteorol. Soc., 75,*** 375-400, 1994.

Platt, C.M.R., and G.R. Patterson, The interpretation of baseline atmospheric turbidity measurements at Cape Grim, Tasmania, *J. Atmos. Chem., 4,* 187-197, 1986.

Reddy, P.J., F. W.Kreiner, J.J. DeLuisi, and Y. Kim, Aerosol optical depths over the Atlantic derived from shipboard sunphotometer observations during the 1988 Global Change Expedition, ***Global Biogeochem. Cycles, 4,*** 225-240, 1990.

Shettle, E.P., and R.W. Fenn, Models for the aerosols of the lower atmosphere and the effects of humidity variations on their optical properties, ***AFGL Rep. TR-79-0214,*** Air Force Geophys. Lab., Bedford, Mass., 1979.

Smirnov, A.V., and Y.N. Gulyaev, The air masses influence on optical characteristics of maritime atmosphere (in Russian), in ***Meteorologicheskie Prognozy (Trudy LGMI),*** edited by V.V. Vorobyev, pp. 110-114, State Polytechnical Institute, Leningrad, 1990.

Smirnov, A.V., and K.S. Shifrin, Relationship of optical thickness to humidity of air above the ocean, ***Izv. Acad. Sci. USSR Atmos. Oceanic Phys.,*** Engl. Transl., ***25,*** 374-379, 1989.

Smirnov, A., A. Royer, N.T. O'Neill, and A. Tarussov, A study of the link between synoptic air mass type and atmospheric optical parameters, ***J. Geophys. Res.,*** 99, 20,967-20,982, 1994.

Vigroux, E., Contribution a l'étude experimentale de absorption de l'ozone, ***Ann. Phys., 8,*** 709-762, 1953.

Villevalde, Y.V., V.V. Yakovlev, and S.P. Smyshlyaev, Measurements of atmospheric optical parameters in Baltic Sea and Atlantic Ocean (in Russian), in ***Issledovaniya Yuzhnoy Chasti Norvezhskogo Moiya,*** edited by E.Y.Kluikov et al., pp. 105-110, Gidrometeoizdat, Moscow, 1989.

Villevalde, Yu.V., A.V. Smirnov, N.T. O'Neill, S.P. Smyshlyaev, and V.V. Yakovlev, Measurement of aerosol optical depth in the Pacific Ocean and the North Atlantic, ***J. Geophys. Res., 99,*** 20,983-20,988, 1994.

Volgin, V.M., O.A. Yershov, A.V. Smirnov, and K.S. Shifrin, Optical depth of aerosol in typical sea areas, ***Izv. Acad. Sci. USSR Atmos. Oceanic Phys.,*** Engl. Transl., ***24,*** 772-777, 1988.

Von Hoyningen-Huene, W., and A. Raabe, Maritime and continental air mass differences in optical aerosol extinction data, ***Beitr. Phys. Atmos., 60,*** 81-87, 1987.

Von Hoyningen-Huene, W., and M. Wendisch, Variability of aerosol optical parameters by advective processes, ***Atmos. Environ., 28,*** 923-933, 1994.

Weller, M., and U. Leiterer, Experimental data on spectral aerosol optical thickness and its global distribution, ***Beitr. Phys. Atmos., 61,*** 1-9, 1988.

Wolgin, W.M., W.F. Radionov, and U. Leiterer, Zur variabilitat der optischen eigenschaften der atmosphare im Nordatlantik, Z. ***Meteorol., 41,*** 267-272, 1991.

N.T. O'Neill, A. Royer, A. Smirnov, A. Tarussov, and Y.Villevalde, Faculte des lettres et sciences humaines, Centre d'applications et de recherches en télédétection (CARTEL), Universitd de Sherbrooke, Sherbrooke, Québec, Canada J1K 2R1. (e-mail: asmirnov@magellan.geo.usherb.ca)

(Received September 19, 1994; revised February 22, 1995; accepted March 24, 1995.)